Elastic All-Optical Networks: A New Paradigm Enabled by the Physical Layer. How to Optimize Network Performances?

Elastic All-Optical Networks: a New Paradigm Enabled by the Physical Layer. How to Optimize Network Performances?

V. Curri, *Member, IEEE*, M. Cantono, *Student Member, OSA*, R. Gaudino, *Senior Member, IEEE*

***Abstract*—A new era for optical networks has been started by the development of transceivers based on digital signal processing (DSP) and operating multilevel modulation formats with coherent and equalized receivers, enabling uncompensated optical links and dynamic transparent wavelength routing in nodes. Connectivity matrices at the physical layer have changed from sparse and *static* to full and *elastic*. So, to fully exploit network potentialities and to implement the elasticity paradigm requested by forecasts of worldwide Internet traffic evolution, the orchestration of logical and physical layer has become a firm requirement. We propose the statistical network assessment process (SNAP) as a method to explore potentialities of physical layer independently of specific traffic allocation. We apply SNAP to a German and to a Pan-EU network topology, first deriving the average bit-rate per lightpath given an any-to-any connectivity matrix – a static metric – in order to compare merits of three typical fiber types and to evaluate benefits of time-domain hybrid modulation formats. Then, assuming physical layer characteristics are set, we perform a SNAP investigation vs. progressive network loading evaluating the blocking probability vs. total allocated traffic – a dynamic metric – with the purpose to compare merits of different size in traffic grooming operating together with multi- or fixed-rate transceivers. We also show how the progressive loading analysis can be used to address selected physical layer upgrades. As an example, we investigate possible upgrades to hybrid Raman/Erbium fiber amplification (HFA) on selected links, then displaying quantitative benefits in terms of enabled excess traffic at a given blocking probability.**

***Index Terms*—WDM networks, Optical fiber networks, SNAP, network design**

I. Introduction

OVER the last decade, backbone optical networks have deeply modified their nature. In legacy networks operated by direct-detection (DD) transceivers, node-to-node links were like sealed data pipelines, and optical-electric-optical (OEO) regeneration in nodes, as well as transparent wavelength routing, were forced to be established in the network design phase, together with dispersion maps in links. Hence, in general, transparency at the logical network level did not meet similar characteristics at the optical transmission level.

With the development of transceivers based on digital signal processing (DSP) and operating multilevel modulation formats with coherent receivers and channel equalization [1], network nodes may now route selected lightpaths (LPs) provided that they maintain the overall LP quality-of-transmission (QoT) above the in-service threshold. Moreover, in state-of-the-art transceivers the delivered modulation format is software-defined by the DSP unit, so multi-rate [2] – *elastic* – devices are able to balance the constellation cardinality – and the corresponding bit-rate – with the lightpath QoT. Consequently, network optical connectivity matrices that in legacy networks operated by DD transceivers were sparse and *static* as they were established during the network design phase, are in modern networks full and *elastic*, i.e., modifiable over a short time-scale. Hence, state-of-the-art optical networks are indeed transparent at every level, and the orchestration [3] of logical and physical layer enables to adapting traffic allocation in order to properly respond to variations in traffic requests over a short time-scale.

In such a novel scenario, every equipment and transmission technique at the physical layer impacts the network behavior. These are, among others, nodes' structure, transmission techniques, spectral use, fiber types, optical amplification and OEO regenerators' placement. Hence, methods giving quantitative evaluations of individual merit of physical layer equipment are a firm request during network design phases as well as during network lifetime, when it is essential for the orchestration of logical and transmission layers and for addressing selected upgrades to properly react to growth and modifications of traffic requests.

Besides enabling transparent wavelength routing, the use of DSP-based transceivers including Rx equalization has dramatically simplified the link structure, removing needs for in-line dispersion-compensating units [4]–[6]. In this transmission scenario, it has been extensively shown that impairments of fiber propagation due to loss, chromatic dispersion, and Kerr nonlinearity can be approximated as an additive Gaussian disturbance on any single frequency, named non-linear interference (NLI) [7]–[16], also in presence of Raman amplification [17]. The amount of NLI can be computed using approximated closed-form expressions displaying excellent accuracy for large spectral occupation, relatively large fiber chromatic dispersion and limited strength of Kerr effect. Characteristics that are indeed *typical* for state-of-the-art optical links. Consequently, a unique parameter determining the QoT of a network LP over a given multi-hop transparent route is the generalized optical signal to noise ratio ($\mathrm{OSNR_{NL}}$), including the accumulation of both the amplified spontaneous emission (ASE) noise introduced by in-line amplifiers and the non-linear interference generated in fiber propagation. In this work, we rely on the the GN-model [15] for the evaluation of $\mathrm{OSNR_{NL}}$,

The Authors are with DET, Politecnico di Torino, Italy (e-mail: vittorio.curri@polito.it).

This work was supported by CISCO Systems within a SRA contract.

supposing full spectral load on each link. Such an assumption corresponds to a worst-case scenario that in any case is not so penalizing, because of the weak dependence of NLI generation with the bandwidth filling and extension [18]. Moreover, we assume networks being operated at the local optimal power spectral density, according to the local-optimization global-optimization (LOGO) control plane [19], [20].

Forecasts [21] for future evolution of Internet traffic envision an overall growth at a compound annual growth rate (CAGR) of 22% until 2020. Besides increasing on the average, demand for IP traffic will become more and more variable with respect to daytime. In particular, busy-hour Internet traffic is envisioned to increase with a CAGR larger than 40%, driven by high-definition video as traffic type, and by mobile traffic as source/destination. Except for the last mile, where 5G wireless technology will be dominant, such a traffic demand will weigh on optical networks, up to large-size regional backbone networks. So, optical networks will have to increase both the average throughput capacity and the flexibility in time, entailing the implementation of the elastic all-optical networks paradigm. On the other hand, network operators aim at maximizing returns on investments done for in-field amplified links [22], limiting as much as possible installation of new equipment. In particular, they aim at exploiting available fibers, limiting upgrades to selected accessible sites as network nodes and amplifiers' sites are. Thus, network operators are starting to implement the elastic paradigm on fixed-grid wavelength division multiplexed (WDM) networks on the C-band, focusing on maximizing link capacity. Later on, they will eventually remove passive filtering components in nodes and will move to flex-grid spectral use, at least for the dynamic busy-hour traffic. Such an evolution will require the adaptation of network management as well as the implementation of selected hardware upgrades, having as constraints the fulfillment of IP traffic growth on one side, and the minimization of costs and of energy consumption on the other.

Merit of transmission components for point-to-point capacity have been extensively analyzed, and fundamental limits have been established as shown for example in [23], while the assessment of networking merits of transmission solutions is still far from being fully developed. The method called statistical network assessment process (SNAP) has been recently proposed [24]–[26] to this purpose: it analyzes a progressive loading of networks according to a defined model for traffic requests and an established routing, spectral and wavelength assignment (RSWA) algorithm. SNAP performs a Monte Carlo analysis (MCA) by generating several realizations of progressive random traffic requests coming from the logical to the optical transmission layer. Requests are allocated up to network saturation according to the given RSWA algorithm, and network status is progressively stored for each generated realization of traffic requests. It enables the estimation of statistics of network metrics both for a given- and for a progressive-traffic loading of networks. SNAP may assume to operate on a completely unloaded topology, or on a network already partially loaded by legacy traffic. Contrary to typical analyses aimed at deriving optimal solutions, given the traffic matrix to be allocated and the knowledge of a strategy to do so, SNAP does not assume such a knowledge *a priori*, so enabling to probe strengths and weaknesses of physical layer solutions independently of specific traffic allocation strategies. SNAP outcomes are both static for a given traffic and dynamic versus loading, so allowing a quantitative comparison of the effectiveness of physical layer solutions both in improving fundamental *capacity* limits and in enhancing performances up to a maximum acceptable blocking. SNAP also drives out weaknesses of networks, as, for instance, links' congestion, consequently addressing specific physical layer and/or RSWA updates.

This paper is the extension of [27] and it is organized as in the following. In Sec. II, we describe the statistical network assessment algorithm, showing how it may deliver statistics of static and dynamic metrics for both given- and progressive-traffic network loading. The latter is the main novelty with respect to [27]. Then, in Sec. III, we present descriptions of the two network topologies – German and Pan-European – considered to derive the results presented in this work. Note that the Pan-European used in the present paper is a simplified version of the one used to derive results of [27] Besides describing details of the physical layer, as fiber type, amplification, and node structure, we also comment on the transmission technologies transceivers are assumed to be based on, and on traffic grooming coming from the logical layer.

In Sec. IV, we describe the analyses we have carried out to compare benefits of fiber types and of times-domain hybrid modulation formats (TDHMF) [28] to implement multi-rate transceivers. These analyses aim at establishing fundamental limits of network topologies when operated in *transparency*, so are focused on metrics computed considering an any-to-any connectivity matrix, in which each connection is operated at the maximum bit-rate allowed by the QoT of the chosen LP on the defined route, given the transmission technique. For this scenario, as unique metric for merit, we propose the average bit-rate per lightpath $R_{b,\lambda}$ for the given connectivity request. We show that TDHMF always overcomes PM-m-QAM, while regarding fiber types, as for point-to-point transmission, best networking performances are always enabled by the pure silica-core fiber (PSCF).

Analyses vs. progressive network loading are described in Sec. V. In particular, we have studied the effectiveness of multi-rate vs. fixed-rate transceivers with different size of traffic grooming on the same couple of network topologies assuming they are made of SMF links. We present results as blocking probability (BP) vs. the total allocated traffic. For the maximum tolerable BP that we assume of 1%, we present results of links' saturation as spectral loading percentage on each node-to-node link, in order to highlight topological network weaknesses and to address specific physical-layer upgrades. To this regard, in Sec. VI, we show an example of upgrades to hybrid Raman/Erbium fiber amplification (HFA) with moderate Raman pumping regime [29] on links with spectral load below 20%. Running SNAP on the updated topologies, we observe an overall traffic improvement at BP = 1%.

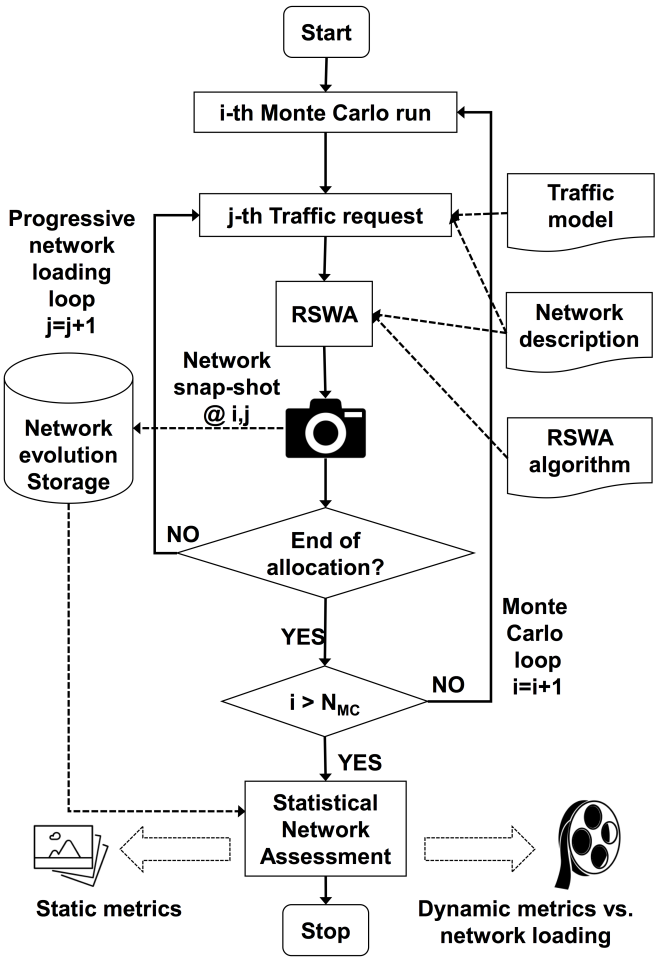

Figure 1. Flowchart for the Statistical Network Assessment Process.

II. Statistical Network Assessment Process

In this section, we introduce the Statistical Network Assessment Process (SNAP). SNAP has been introduced and used in [24]–[26], and it is an algorithm to statistically characterize the strengths and weaknesses of the physical layer in reconfigurable optical networks. The flowchart of Fig. 1 describes SNAP. SNAP is a Monte Carlo based algorithm that makes use of the following input information during each different Monte Carlo iteration.

1) Traffic model description. Depending on the selected traffic model, SNAP can be used to perform given-traffic or progressive-traffic analyses as described in the following.
   - Given-traffic analysis.
     A traffic matrix D is defined, in which each element $D_{l,m}$ may represent either a connections' request or a bidirectional data-rate request between nodes l and m. In the former case, the element $D_{l,m}$ serves as the number of LPs to be allocated between nodes l and m. In the latter, it is a request for transport between node l and m of *groomed* traffic of size R_G expressed in Gbps that the physical layer is expected to satisfy according to the supposed transceiver – fixed- or multi-rate – technology and spectral use – fix- or flex-grid – method. For the given-traffic analysis the randomness – Monte Carlo loop in Fig. 1 – is in the order the elements $D_{l,m}$ are considered, and the network loading loop ends when all $D_{l,m}$'s are considered by the RSWA algorithm. This analysis is more suitable for derivation of static metrics from network status at the end of every loading loop.
   - *Progressive-traffic* analysis.
     In this case, the traffic model generates requests evolving indefinitely with the progressive loading loop on j of Fig. 1. So, the model is indeed a traffic distribution, namely a bivariate probability mass function in the source/destination node space, expressing the probability that a request for connection between two nodes might occur at j. As for the given-traffic analysis, the type of request can be either a LP-connectivity without rate-size or a data-rate request. For the latter, the request size can be either fixed and defined by the traffic grooming at the logical level, or randomly generated according to a specific probability density function. For this analysis the loop on network loading terminates at network saturation, i.e., when several subsequent requests for connection are blocked. This kind of traffic model is suitable for the estimation of both static and dynamic metrics, as at the end of the Monte Carlo loop we can either derive statistics for each loading level or at saturation.
2) A full description of network topology and physical layer. For topology definition we consider number of nodes, connectivity and preexisting network loading due to possible legacy traffic. While, as physical layer characteristics we take into account fiber type, amplification method, control planning, available bandwidth, fix- or flex-grid spectral use, grid size, and transceiver characteristics and placement. Physical layer parameters are needed to compute the figure of merit for QoT of each lightpath, i.e., the generalized optical signal to noise ratio via the GN-model [15].
3) Characteristics of the Routing and Spectrum/Wavelength Assignment (RSWA) algorithm, i.e., the routing policy. Namely, the way in which fiber paths between nodes' pairs are computed and ranked and spectral slots assigned to LPs. For example, a shortest link or smallest number of hops routing could be adopted.

During each Monte Carlo iteration, the network is loaded according to the traffic model of choice as in the following. In case of given-traffic analyses, the order of requests for traffic allocation is shuffled and each of them is tentatively allocated according to the selected RSWA, exploiting the analyzed transceiver technology and spectral use defined in the network description. For each Monte Carlo loop, the allocation ends when the full list of demands has been considered. For *progressive-traffic* analyses, traffic between random source-destination pairs is generated and tentatively allocated. In such

case the allocation process ends either when the network is fully saturated, or a maximum number of consecutive missed allocations is reached. For both types of analyses several networks metrics can be computed and stored at each j-th tentative allocation during each i-th Monte Carlo run. Among others, the set of metrics may include the ones listed and described in the following.

- The average bit-rate per lightpath $R^i_{b,\lambda}$ that is given by

$$R^i_{b,\lambda} = \frac{1}{N_{L,i}} \sum_{n=1}^{N_{L,i,j}} R_{b,n} \quad \text{[Gbps]} \tag{1}$$

  where $N_{L,i,j}$ is the number of allocated lightpaths during the i-th Monte Carlo run up to the j-th demand and $R_{b,n}$ is the bit-rate of the n-th allocated LP.
- Details about spectral occupation of each node-to-node fiber connection.
- Blocking information such as the number of blocked demands for each node or link.
- Acceptance information such as the number of demands accepted in each node.

The set of metrics to be considered can be modified in order to target specific alternative network aspects. In this sense, SNAP can be easily extended providing a relevant flexibility in the characterization process. Due to the traffic randomization, the allocation process of each Monte Carlo run may differ from previous runs, thus the output results of each run will be – in general – stochastic.

After the maximum number of Monte Carlo iterations N_{MC} has been reached, each metric can be statistically characterized with respect to the random traffic generation or scrambling. This means that the probability density functions (PDF) of each analyzed metric can be derived, thus obtaining a *statistical* insight on network capabilities and critical aspects. Statistics of network metrics can be used to derive *probabilistic* information on network performances, such as the probability that the spectrum of a given link will be saturated over a certain percentage, *independently* on how traffic will be allocated on the network. Although Monte Carlo based algorithms have already been used in network analyses [30]–[32], to the best of our knowledge, the approach proposed in [25] and exploited and refined in this paper is original and innovative. In addition to this, exploiting SNAP one can focus on the statistics of results either at the end of the allocation processes, thus obtaining *static* metrics representing the network status, or versus the loading evolution in order to obtain a *dynamic* representations of network conditions. Both analyses can be performed independently from the traffic type, but in general the *dynamic* one is more relevant in case of progressive-traffic due to the larger number of demands that are generated in that case. Similarly, the given-traffic case is more likely to be analyzed considering static metrics. In this paper we consider both kinds of metrics representations, applying the static ones to a given-traffic analysis and the dynamic one to a progressive-traffic scenario.

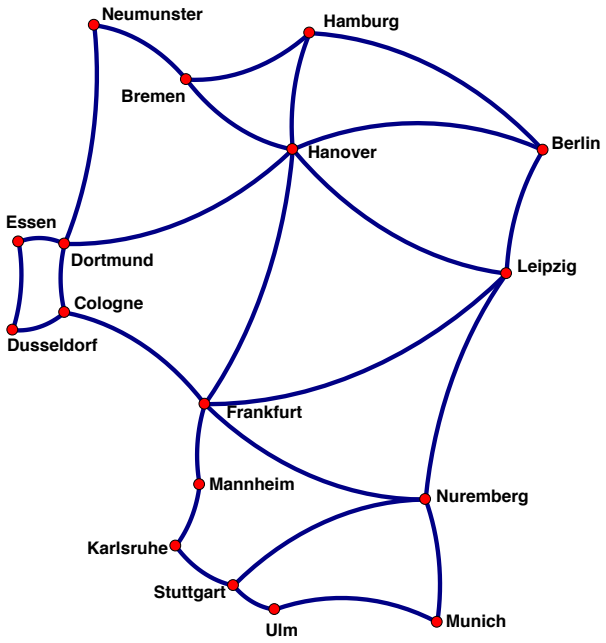

(a) German topology - 17 nodes, 26 links, average link length 207 km, average node degree 3.06.

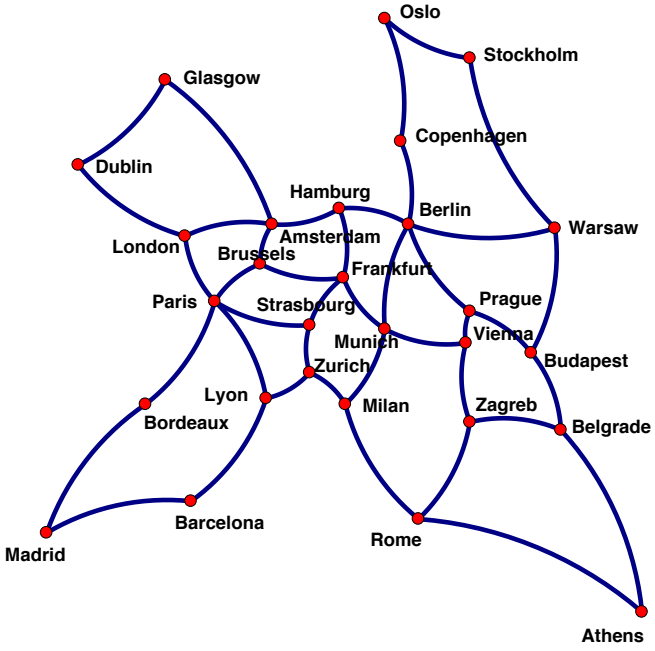

(b) Pan-European topology - 28 nodes, 41 links, average link length 637 km, average node degree 2.93.

Figure 2. Considered network topologies.

III. Analyzed Network Scenarios

In this paper, we analyze the two network topologies depicted in Fig. 2. These refer to a German network made of 17 nodes and 26 links with average link length of 207 km (Fig. 2a), and average node degree of 3.06, and to a Pan-European network topology made of 28 nodes and 41 links with average link length of 637 km and average node degree 2.93 (Fig. 2b). In both cases, we assume the amplified node-to-node fiber links to be in pairs, providing bidirectional connectivity between nodes such that networks are considered

Fiber Type	Loss α_{dB} [dB/km]	Dispersion D [ps/(nm · km)]	Effective Area A_{eff} [μm^2]
NZDSF	0.220	3.8	70
SMF	0.200	16.7	80
PSCF	0.167	21.0	135

Table I
MAIN FIBER CHARACTERISTICS FOR THE THREE FIBER TYPES CONSIDERED FOR THE GIVEN-TRAFFIC ANALYSIS.

as undirected graphs. We assume uniform, uncompensated and amplified fiber links with lumped EDFAs fully recovering fiber losses and characterized by a noise figure of 5 dB. For the given-traffic analysis, we consider networks to be possibly made of three different *typical* fiber types: SMF, NZDSF and PSCF, whose main characteristics are summarized in Tab. I. For all three fiber types we assume a non-linear index coefficient $n_2 = 2.5 \cdot 10^{-20}$ m^2/W, yielding nonlinear coefficients γ: 1.25 W^{-1}km^{-1}, 1.47 W^{-1}km^{-1}, 0.75 W^{-1}km^{-1} for SMF, NZDSF and PSCF, respectively. Each fiber span is assumed to operate propagating channels at the optimal power spectral density computed by means of the incoherent GN-model as prescribed by the LOGO strategy for control planning [19], [20], assuming full spectral load of each link.

We suppose all nodes to be equipped with Reconfigurable Add-Drop Multiplexers (ROADMs) introducing a routing loss of 18 dB, that is fully recovered with an additional EDFA at the output of nodes. We do not consider any further impairment on channel spectra caused by filtering effects of ROADMs. We assume that the physical layer operates WDM transmission on the C-band set to B_{opt} = 4 THz exploiting the 50 GHz ITU-T fix-grid, consequently enabling a maximum of $N_{\text{ch}} = 80$ lightpaths – channels at given wavelengths – per fiber.

We select as RSWA algorithm a k_{max}-best-OSNR based routing policy with first fit wavelength assignment. This means that paths between a nodes' pair are computed by using a k-shortest-path algorithm, in which the best k_{max} paths in terms of QoT, i.e., lowest OSNR$_{\text{NL}}$ degradation, are considered as suitable paths for LPs. In particular, k_{max} represents the number of different paths between nodes' pairs that can be used to find available wavelengths to accommodate routes for LP demands. The considered RSWA selects the path and the wavelengths on a first fit basis, searching for wavelengths in higher QoT paths first, then moving to lower QoT paths if no available wavelengths in higher QoT paths are found. Since we consider the generalized OSNR as QoT for LPs, including both the accumulated ASE noise and NLI, to compute best-OSNR routes, we use the incoherent GN-model as described in details in [25]. For our analyses we tuned k_{max} and set it to 50. We use such a wide set of routing space, so as to consider low QoT routes and exploit the tuning capabilities of the multi-rate transceivers described in Sec. V and increase the total network traffic that can be sustained by the network.

IV. GIVEN-TRAFFIC ANALYSES

The first SNAP analyses we have performed are given-traffic investigations aimed at deriving the average bit-rate per lightpath $R_{b,\lambda}$ as *static* metric for physical layer solutions. As

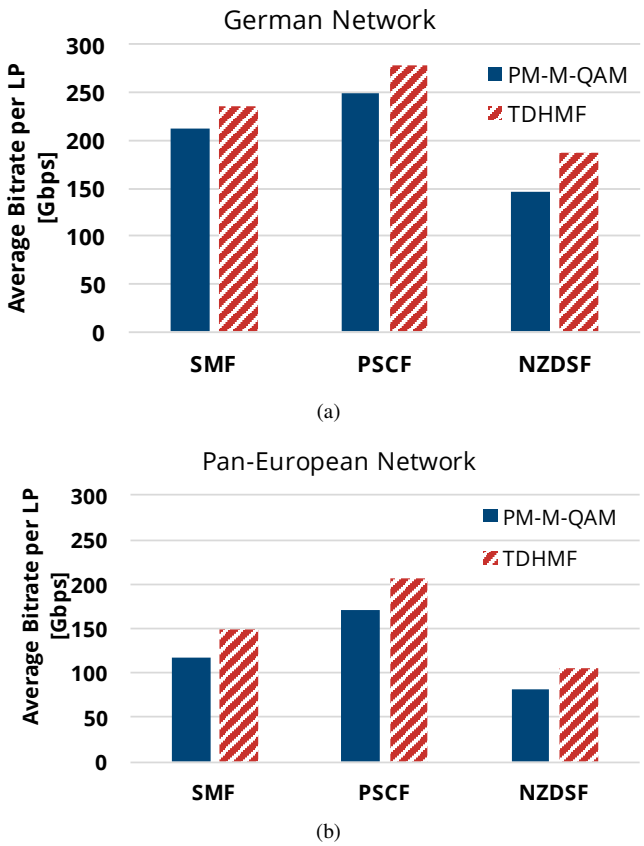

Figure 3. Average bit-rate per lightpath for given-traffic analyses using different fiber types and different multi-rate transceivers for the German (a) and Pan-EU (b) network topologies.

traffic model we have considered an any-to-any connectivity matrix D, i.e., $D_{l,m} = 1 \ \forall \ l, m$ and $D_{l,m} = 0$ for $l = m$. Using such an approach we compare networking merit of the three different *typical* fiber types of Tab. I, and of hybrid- vs. pure-format solutions to implement multi-rate transceivers.

For the analyzed scenarios, we heuristically estimated as $N_{\text{MC}} = 5000$ the number of Monte Carlo iterations needed to give a reliable evaluation of network statistics. At every i-th Monte Carlo iteration, a different random *realization* of the evolution vs. j of LP requests is generated, according to the considered any-to-any connectivity.

At the end of the i-th random allocation we compute the average bit-rate per LP $R^i_{b,\lambda}$ for that *realization* by averaging the bit-rate that each allocated LP can achieve as described by Eq. 1. At the end of the MCA, the set of N_{MC} realizations of $R^i_{b,\lambda}$ is available, enabling to estimating the related probability density function (PDF). Then, to obtain a unique *static* metric of network performance given the physical layer characteristics, we evaluate the average $R_{b,\lambda}$ of the PDF.

We consider two different options for the implementation of multi-rate transceivers. One is based on *pure* modulation formats – polarization multiplexed (PM) m-QAM constellations – enabling to delivering a finite and discrete set of rates, corresponding to the PM-m-QAM constellation enabled by the QoT of the considered LP on the established route. The alternative option exploits TDHMFs [28] and enables to

adjusting with continuity the delivered rate to the QoT of the considered LP on the established route. For both options, we suppose to rely on modulation formats with *squared* constellations, i.e., PM-BPSK, PM-QPSK, PM-16-QAM, and PM-64-QAM, for which data flows are independent on each of the four *quadratures*. Hence, spectral efficiency varies in [2,4,8,12] as Bit per Symbol (BpS) according to the QoT in case of *pure* modulation formats, while BpS may adapt with continuity from 2 to 12 to the QoT when we rely on TDHMF transceivers. We consider state-of-the-art DSP units able to manage a *gross* data symbol rate $R_{s,g} = 32$ GBaud per lightpath, corresponding to a net symbol rate $R_s = 25$ GBaud per lightpath due protocol and coding overhead that we assume to be of 28%. So, we suppose LPs are *in-service* on the assigned routes if the pre-FEC BER $\leq 4{\cdot}10^{-3}$, and consequently evaluate the scaling of transceiver rate with the available QoT, given by OSNR_{NL} [28]. Therefore, net bit rates and required OSNR in 0.1 nm are 50 Gbps and 9.5 dB for PM-BPSK, 100 Gbps and 12.6 dB for PM-QPSK, 200 Gbps and 19.2 dB for PM-16QAM, and 300 Gbps and 25.1 dB for PM-64QAM respectively. For TDHMs, net bit rates may scale from 50 up to 300 Gbps according to a lightpath OSNR in 0.1 nm from 9.5 dB up to 25.1 dB. For details, please refer to [28].

Fig. 3a and Fig. 3b show results obtained for the German and the Pan-EU topology, respectively. These figures display for each fiber-type, $R_{b,\lambda}$ enabled by PM-m-QAM and TDHMF, as filled and stripped bars, respectively. Focusing on merit of fibers, it can be noted that, for both topologies, the fiber-type hierarchy established for point-to-point transmission [18] holds also at a network level: PSCF delivers the best performance, followed by SMF and NZDSF, respectively, independently of the adopted transceiver configuration. Taking SMF as a reference, benefits brought by PSCF are much larger on the Pan-EU topology [1] – 44.9% and 38.4% for PM-m-QAM and TDHMF, respectively – than on the German one – about 17%, independently of the transmission technique. For NZDSF, relative $R_{b,\lambda}$ penalty with respect to SMF is always around 30% except for the German topology operated by TDHMF for which a penalty limited to 20.8% can be observed. Differences in merit of PSCF vs. SMF among the two topologies are related to the different average link length. In the smaller extension German topology distances are shorter, and consequently, LPs are characterized by a better QoT, enabling a larger rate, also in case of using the poorer transmission quality SMF. But the maximum bit-rate is limited to 300 Gbps per LP for both transceiver options, so potentialities of the higher transmission quality PSCF are *clipped*, in case many LPs are enabled to operate the maximum bit-rate already using the SMF, thus causing a compression of the bit-rate distribution towards large values. Therefore, the advantage of PSCF over SMF is smaller in the German topology than in the Pan-EU case. For the disadvantage of NZDSF with respect to SMF, a general tendency driven by the topology cannot be observed because the stronger NLI generation, caused by the smaller dispersion and effective area, does not allow to approach the maximum bit-rate of transceivers.

Comparing the two options for multi-rate transceivers, TDHMF always outperforms PM-m-QAM thanks due to the better exploitation of the available OSNR_{NL} on LPs. The relative $R_{b,\lambda}$ advantage of TDHMF over PM-m-QAM varies from 11% to 28%, depending on the topology and on the fiber type. On the Pan-EU topology, TDHMF outperforms PM-m-QAM of 20% with PSCF, of 26% with SMF, and of 28% with NZDSF, while for the German network, relative advantages of TDHMF are of 12% for both PSCF and SMF, and of 28% for NZDSF. A general tendency of TDHMF advantages with respect to fiber type can be observed: the poorer the fiber quality in transmission, the higher the advantage of TDHMF. Such a behavior is caused by the better capability of TDHMF in exploiting QoT of LPs that is more effective when the physical layer of the considered scenario does not allow to approach the maximum bit-rate, i.e., in case of poorer transmission quality fiber in larger-size networks. In smaller-size networks, as the German topology is, for fibers permitting to approach the maximum bit-rate of 300 Gbps/LP the *clipping* effect takes place, limiting the relative advantage of TDHMF with respect to PM-m-QAM to 12% for both SMF and PSCF scenarios. On the other hand, for the poorer transmission quality NZDSF scenario, clipping does not occur, hence the relative advantage of TDHMF vs PM-m-QAM is 28% for both considered topologies.

V. Progressive-Traffic Analyses

In this section we describe the progressive-traffic analyses we have carried out applying SNAP to the German and Pan-EU network topologies of Fig. 2, targeting the estimation of *dynamic* metrics as the blocking probability and links' saturation vs. the total progressively allocated network traffic. In this case, we do not target the comprehension of the merit of fiber types, so we suppose for both networks node-to-node links uniformly made of amplified SMF fiber pairs.

For traffic modeling, we assume that requests generated at every j-th iteration of the network loading loop of SNAP are random and uniformly distributed among nodes. It means that the probability of getting a request for data connection between two nodes is constant and equal to $1/[N_{\text{nodes}}(N_{\text{nodes}} - 1)]$ for each nodes' pair, for each j. N_{nodes} is the number of network nodes generating and receiving traffic. We assume traffic requests to be defined by the traffic-grooming size R_G, being either 100 Gbps or 200 Gbps for each connection requested between two nodes. The comparison of the merit of the two considered R_G values is performed together with the evaluation of the merit of two different transceiver structures. To this regard, we consider the multi-rate transceivers based on PM-m-QAM *pure* modulation formats as already described and analyzed in Sec. IV. So, this type of transceivers is able to deliver a net bit-rate of 50, 100, 200 and 300 Gbps, depending on the OSNR_{NL} of the selected LP on the established route. As a comparison, we take into account fixed-rate transceivers based on PM-QPSK, delivering 100 Gbps, or exploiting PM-16-QAM, operating LPs at 200 Gbps. As target pre-FEC BER

[1]Note that the analyzed Pan-EU topology is a simplified version of the the one used in [27].

we consider the same value of 4×10^{-3} as for the given-traffic analyses of Sec. IV. For multi-rate transceivers we assume the capability of splitting the traffic on more than one LP, if the available LPs are not able to enable a bit-rate large enough to meet the considered traffic-grooming size, due to low QoT.

For these analyses we targeted the observation of performances down to a blocking probability of 0.1%, so we estimated $N_{\mathrm{MC}} = 10000$ to be the number of Monte Carlo iterations needed to perform a proper statistical evaluation of dynamic metrics. Moreover, in this case, traffic is not limited, so we had to establish exit conditions for the network loading loop of SNAP. To this purpose, we defined to perform random progressive allocations up to the network status for which more than 5000 requests have been generated and more than 50% of them is blocked.

This progressive-traffic analysis aims at evaluating the dynamic metrics described in the following.

- *Blocking probability* (BP), that is the probability of demand $j+1$ being blocked after demand j. BP expresses the Grade-of-Service (GoS) of the network under progressive loading.
- Total allocated network traffic computed by summing the number of allocated requests up to the j-th demand. Selecting a target GoS, one can evaluate the average maximum traffic that the network can sustain at that target GoS.
- Links' saturation, i.e., the number of the occupied wavelength channels over the total available bandwidth in each network link.

Being SNAP a framework for Monte Carlo analyses, results are indeed PDFs of targeted metrics, so, as for given-traffic results, also in this case we summarize results as the *evolution* of the average of considered metrics with progressive loading of networks.

Fig. 4a represents the growth of average BP vs. average total allocated network traffic for two different grooming values and the fixed- or multi-rate transceivers for the German topology. As it can be expected, BP progressively grows as the network is increasingly loaded by allocating random traffic requests. The smaller-size German topology, when operated with a traffic grooming of 200 Gbps achieves better performances than for smaller grooming size of 100 Gbps, independently of the transceiver configuration. This is due to physical layer characteristics and to the network size enabling an average QoT of LPs that is well matched to 200 Gbps requirements: operating with smaller request entails a waste of network achievable throughput close to 50%. This is also corroborated by considering results of Sec. IV, Fig. 3a, where it was shown an average bit-rate per LP slightly higher than 200 Gbps for the SMF-made German topology. Moreover, it can be noted that the multi-rate transceivers do not enable benefits with respect to the fixed-rate ones since a very small number of requests have to be split into multiple channels due to QoT constraints. The vast majority of requests can be transparently carried using PM-16QAM, delivering 200 Gbps per LP. Always referring to Fig. 4a, setting a GoS-BP level equal to 1%, the average maximum achievable network throughput up to that BP value can be evaluated. In case of 100 Gbps grooming this

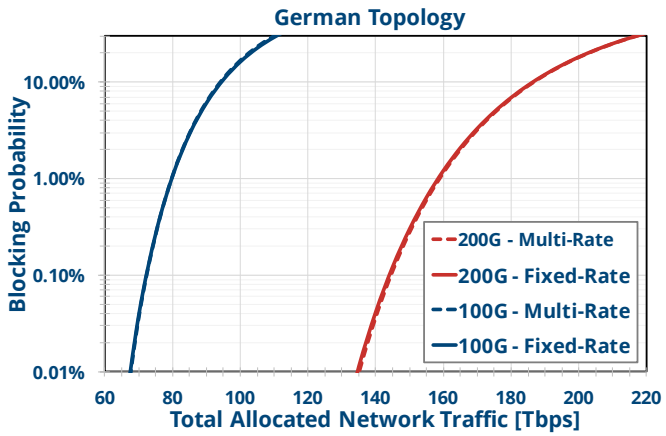

(a) Average blocking probability vs. average total allocated network traffic

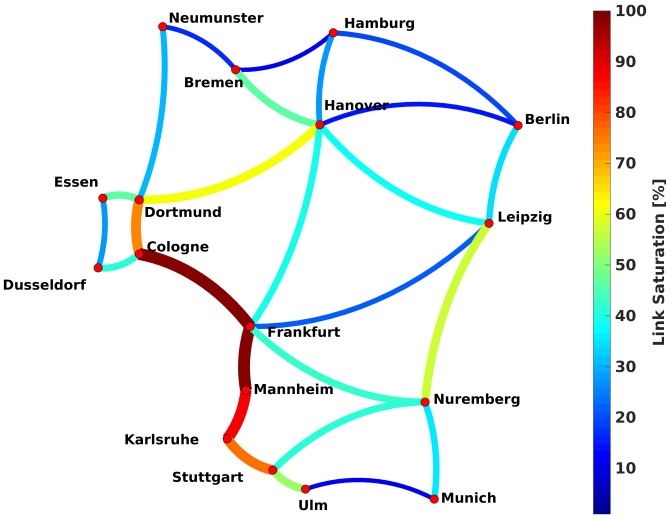

(b) Average links' spectral load at BP = 1%. The ticker the lines the more saturated the links.

Figure 4. Progressive-traffic results for the German topology.

value is around 80.5 Tbps, whereas for $R_G = 200$ Gbps it is 160.3, quantitatively confirming that in this case a grooming of 100 Gbps implies a wasting of almost 50% of the total network throughput.

Fig. 4b depicts the average link saturation obtained at GoS-BP of 1% for 200 Gbps grooming and multi-rate transceivers. Note that this is a static result, but from SNAP outcomes, one could observe the animated representation showing how links progressively saturate on average as network gets increasingly loaded. Referring to Fig. 4b one can immediately identify some of the network striking features and critical aspects. Notice for example the high average saturation of the eastern links (from Cologne to Stuttgart) and the low saturation of the northern ones (from Neumunster to Hamburg). These pieces of information can convey advice to network designers and operators: western links are more critical in terms of reliability since they carry a large percentage of total network traffic; the northern ones are scarcely used since they are penalized in routing ranks due to their higher OSNR degradation, thus they should be improved at the physical layer. Such kind of analyses and considerations allow therefore to shed light on the merit of physical layer on networking performances and

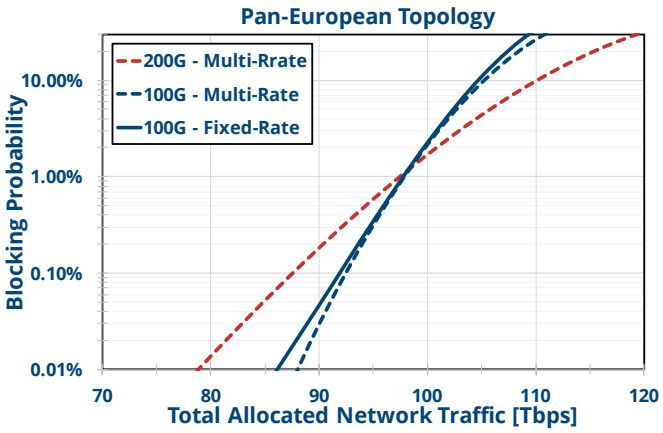

(a) Average blocking probability vs. average total allocated network traffic

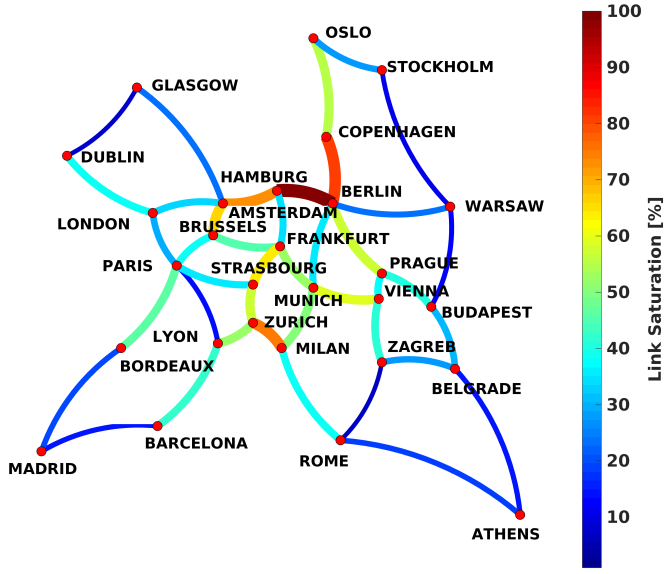

(b) Average links' spectral load at BP = 1%. The ticker the lines the more saturated the links.

Figure 5. Progressive-traffic results for the PAN-EU topology.

crucial facets, creating a strong support for physical layer-driven network upgrade and design strategies. An example of this will be described in Sec. VI.

Fig. 5a shows average BP vs. average total allocated network traffic for the Pan-European topology.

Notice that the curve for the case of $R_G = 200$ Gbps and fixed-rate transceivers is not shown, since a very small portion of LPs have QoT large enough to be operated by PM-16QAM yielding for this case a high average BP larger than 50% already for limited traffic. In general, for this topology, 200 Gbps, and 100 Gbps grooming sizes cannot be ranked in a univocal way. For BPs smaller than 1%, 100 Gbps grooming with fixed and multi-rate transceivers can guarantee better performances than 200 Gbps grooming. As BP increases, this ranking is reversed: for higher blocking, requests groomed at 200 Gbps operated via multi-rate transceivers permit to achieve a higher throughput, on average. The explanation for such a behavior is that for very low BP, QoT of LPs is dominant with respect to wavelength availability: in the low BP regime, LPs are blocked only when they cannot be allocated due to QoT constraints because the average network saturation is still very low and plenty of wavelengths are available. In such a scarcely-loaded network status, 200 Gbps requests are more likely to be blocked due to QoT constraints rather than 100 Gbps requests, that are less OSNR demanding. In the high BP regime we are facing an heavily-loaded network, so wavelength blocking becomes dominant with respect to QoT blocking, and both 100 and 200 Gbps requests will have similar blocking probabilities. However, since 200 Gbps requests carry a traffic that is double with respect to 100 Gbps, 200 Gbps will enable a higher allocated network traffic in such high BP regime, thus reversing the low-BP ranking. The crossing point between the two regimes is close to BP = 1%, for which the average total allocated network traffic is around 98.3 Tbps.

Fig. 5b represents the average link saturation of the Pan-EU topology obtained at GoS-BP of 1% for 200 Gbps grooming and multi-rate transceivers. Once again, network most critical links can be identified: in such case links of the northern-EU area connecting Hamburg, Amsterdam, Berlin and Copenhagen are more saturated than the others. At the same time, the most peripheral ones are less used, once again due to the large OSNR degradation they introduce. In Sec. VI, some possible upgrades derived from these progressive-traffic analyses are presented.

VI. SNAP-driven network upgrades: selective HFA introduction

In this section, starting from the quantitative and qualitative evidence of Fig. 4b and Fig. 5b we evaluate the impact of selective upgrades to the amplification equipment to enhancing QoT of underutilized links. In particular, we upgrade links whose saturation is lower than 20% to Hybrid Erbium/Raman fiber amplification (HFA), to reduce ASE noise thus enhancing the QoT of the links. We assume to use HFAs in the moderate pumping regime enabling equivalent noise figures down to 0 dB while avoiding Raman pump depletion [18] and relevant NLI enhancement with respect to lumped amplification. The number of links upgraded in the German topology is 5, whereas it is 9 for the Pan-European topology, as it is reported in the blue histograms of Fig. 8. After applying the selected upgrades, we re-run SNAP to verify variations in BP vs total allocated network traffic curves. Results are reported in Fig. 6 and Fig. 7, for the German and Pan-EU topology, respectively. Whereas the red and white striped histograms of Fig. 8 show the average saturation per link at BP=1%, compared to results before the upgrade (filled histogram).

Referring to results for the German topology of Fig. 6a and Fig. 6b, it can be noted that selectively upgrading to HFA 5 links out of 26, enables an improvement in average total allocated network traffic at BP = 1% of 4%, moving from 160.1 Tbps to 166.3 Tbps. This relatively modest increase is mainly due to the high spectral saturation of links between Cologne and Karlsruhe. The lack of available wavelengths in these links creates a bottleneck for new requests, that are blocked because of absence of alternative routes with adequate QoT. In order to solve such issue and to enable

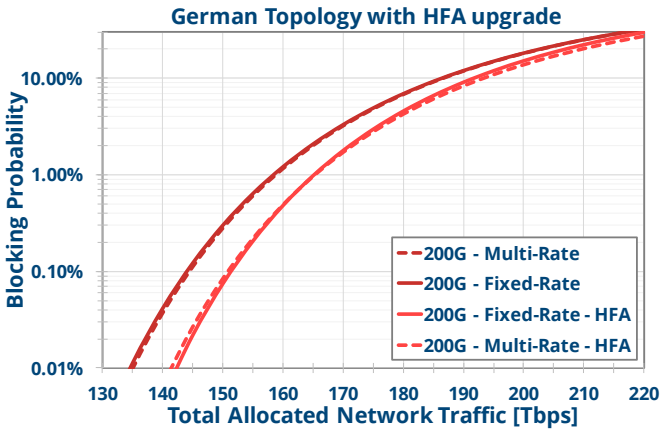

(a) Average blocking probability vs. average total allocated network traffic

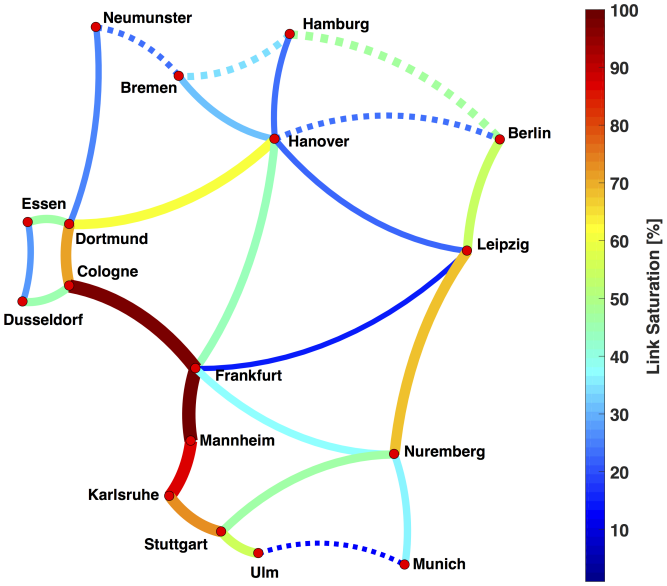

(b) Average links' spectral load at BP = 1%. The ticker the lines the more saturated the links. Dashed lines indicates HFA-upgraded links.

Figure 6. Progressive-traffic results for the German topology post HFA upgrade.

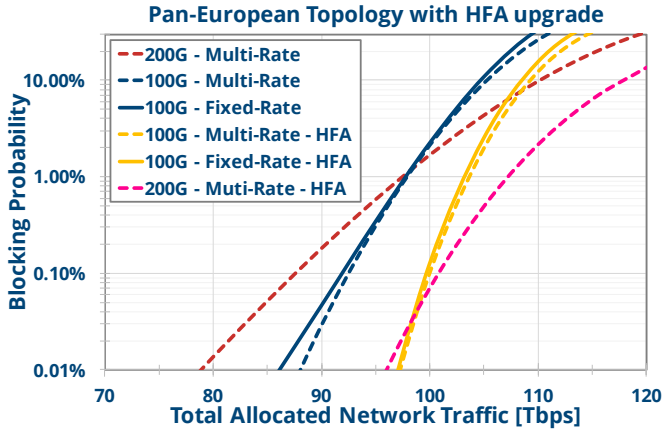

(a) Average blocking probability vs. average total allocated network traffic

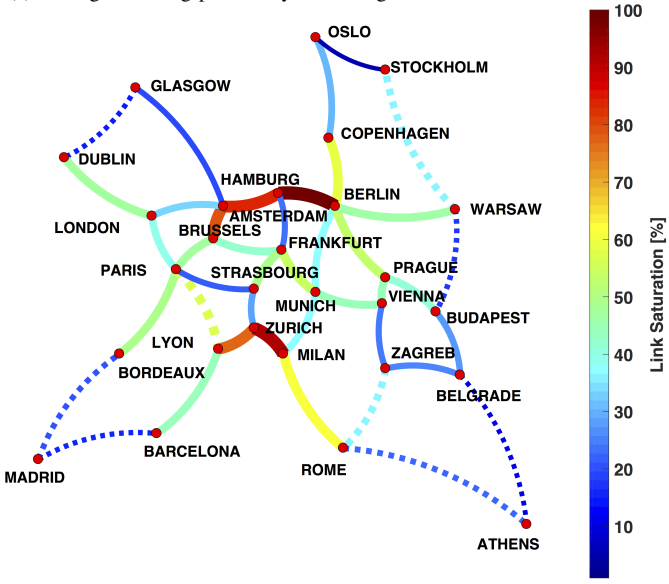

(b) Average links' spectral load at BP = 1%. The ticker the lines the more saturated the links. Dashed lines indicates HFA-upgraded links.

Figure 7. Progressive-traffic results for the Pan-Eu topology post HFA upgrade.

larger improvements, bottlenecks must be removed either: (i) by applying spatial-division multiplexing (SDM) on the highly saturated links by lighting up new fiber pairs, or (ii) by upgrading the amplification technology in more underutilized links (e.g., Frankfurt to Leipzig). Referring to Fig. 6b, it can be observed that the HFA upgrade is useful in increasing the saturation of the northwest links of the German network, but the effectiveness drops for the southern links due to the aforementioned bottleneck.

Fig. 7 refers to the upgraded Pan-European network scenario, where 9 links out of 41 have been selected for HFA upgrade. Observing Fig. 7a, it can be noted how selective upgrades in the amplification technology enable an increase in average total allocated network traffic of 5% and 9% for fixed and multi-rate transceivers with $R_G = 100$ Gbps and for multi-rate transceivers with $R_G = 200$ Gbps, respectively. It can be noticed that the crossing point between the two grooming sizes moves down close to 0.01% thanks to HFA upgrading. This is enabled by increased QoT in several network LPs, allowing to transmit more 200 Gbps requests using single PM-16QAM-operated LP allocations, thus increasing the overall spectral efficiency and the network capacity. As far as link saturation is concerned, it can be noted that some of the previously under-utilized links are now more heavily used, thanks to an improved traffic distribution among links enabled by the increase in availability of high-QoT paths. Similarly to German topology, to further improve network capacity one could also consider SDM-based solutions to remove bottlenecks, or further upgrades to physical layer equipment to guarantee an increased QoT in low-OSNR links. Also for these possible alternative upgrades, SNAP analyses are able to address and to evaluate benefits of these physical layer improvements.

VII. Comments and Conclusions

We have proposed the Statistical Network Assessment Process as a methodology to quantitatively evaluate networking

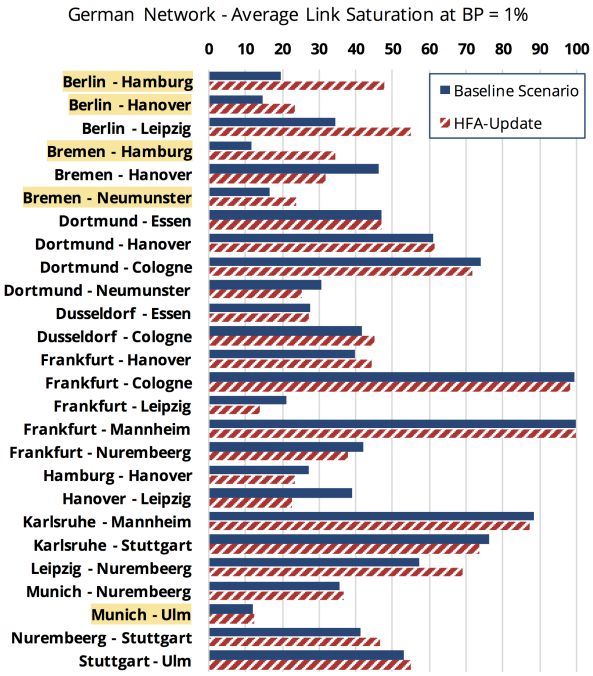

(a) German Topology

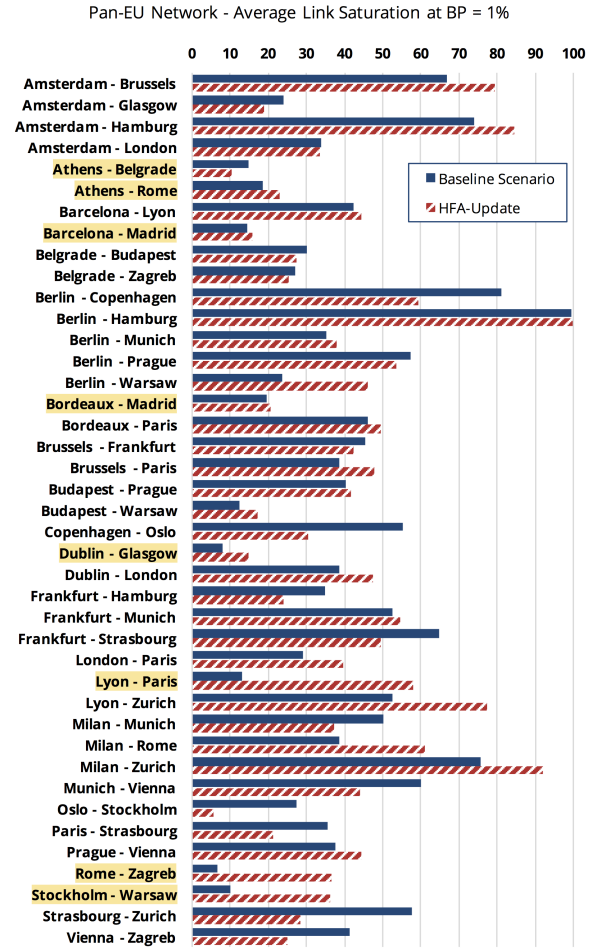

(b) Pan-European Topology

Figure 8. Average link spectral saturation at BP=1% pre and post-HFA upgrades. Yellow labels highlight HFA-upgraded links.

merits of physical layer technologies in reconfigurable transparent optical networks, independently of predefined traffic loads. Such an approach is needed in order fully exploit network potentialities and to implement the elasticity paradigm through the orchestration of logical and physical layer. Moreover, we have shown how SNAP may highlight weaknesses and strengths of a given network topology in order to drive design choices or to address selected updates.

As an example of SNAP use, we have analyzed two regional-network of different size: a German topology as a medium-size and a Pan-EU topology as a large-size. For both topologies, we have performed given- and progressive-traffic analyses. Given traffic analyses have been performed allocating a randomly shuffled any-to-any connectivity in order to measure benefits in terms of average bit-rate per lightpath – a *static* metric – of three *typical* fiber types and of two different techniques for the implementation of multi-rate transceivers – TDHMF or *pure* PM-m-QAM. We have displayed that networking ranking of fibers follows the point-to-point hierarchy – the larger the dispersion, the better – but quantitative benefits depend on the topology and on transmission techniques. We have shown that TDHMF always overcomes PM-m-QAM with an $R_{b,\lambda}$ advantage from 11% to 28%, depending on the topology and on the fiber type, with benefits that are bigger for larger-size topologies and for poorer transmission quality fibers.

We have also applied SNAP to carry out progressive-traffic analyses in order to derive *dynamic* metrics measuring the Quality-of-Service vs. the progressive and uniformly random network load, as the blocking probability vs. the total allocated network traffic. Using these analyses, we have tested two different traffic-grooming sizes – 100 Gbps and 200 Gbps – together with the use of fixed- or multi-rate transceivers. For the smaller-size German topology the best option is grooming size of 200 Gbps and fixed-rate transceivers, while for the larger-size Pan-EU topology performances with grooming of 200 Gbps with multi-rate transceivers correspond to the ones of 100 Gbps with fixed-rate transceivers, at BP = 1%. Furthermore, we have shown how progressive-traffic analyses are able to drive out topology bottlenecks through the links' saturation heat maps, and to consequently address selected updates, as, for instance, amplification update in underutilized links inducing large OSNR penalty, or SDM implementation in highly congested links. To this regard we have shown a strategy to select links for HFA amplification update and we have re-analyzed network topologies supposing such an update was implemented. Thanks to the SNAP outcomes, we have observed an overall traffic improvement enabled by selected HFA updates of 4% and 9% for the German and Pan-EU topology, respectively.

REFERENCES

[1] D. S. Ly-Gagnon *et al.*, "Coherent detection of optical quadrature phase-shift keying signals with carrier phase estimation," *J. Lightw. Technol.*, vol. 24, no. 1, pp. 12–21, Jan 2006.

[2] D. Rafique *et al.*, "Multi-Flex Field Trial over 762km of G.652 SSMF Using Programmable Modulation Formats up to 64QAM," in *Optical Fiber Communication Conference*. Optical Society of America, 2016, p. W4G.2. [Online]. Available: http://www.osapublishing.org/abstract.cfm?URI=OFC-2016-W4G.2

[3] R. Muñoz *et al.*, "Transport Network Orchestration for End-to-End Multilayer Provisioning Across Heterogeneous SDN/OpenFlow and GMPLS/PCE Control Domains," *J. Lightw. Technol.*, vol. 33, no. 8, pp. 1540–1548, April 2015.

[4] V. Curri *et al.*, "Dispersion Compensation and Mitigation of Nonlinear Effects in 111-Gb/s WDM Coherent PM-QPSK Systems," *IEEE Photonics Technology Letters*, vol. 20, no. 17, pp. 1473–1475, Sept 2008.

[5] G. Gavioli *et al.*, "100Gb/s WDM NRZ-PM-QPSK long-haul transmission experiment over installed fiber probing non-linear reach with and without DCUs," in *2009 35th European Conference on Optical Communication*, Sept 2009, pp. 1–2.

[6] D. van den Borne *et al.*, "POLMUX-QPSK modulation and coherent detection: The challenge of long-haul 100G transmission," in *2009 35th European Conference on Optical Communication*, Sept 2009, pp. 1–4.

[7] A. Bononi *et al.*, "Modeling nonlinearity in coherent transmissions with dominant intrachannel-four-wave-mixing," *Opt. Express*, vol. 20, no. 7, pp. 7777–7791, Mar 2012. [Online]. Available: http://www.opticsexpress.org/abstract.cfm?URI=oe-20-7-7777

[8] A. Carena *et al.*, "Modeling of the Impact of Nonlinear Propagation Effects in Uncompensated Optical Coherent Transmission Links," *J. Lightwave Technol.*, vol. 30, no. 10, pp. 1524–1539, May 2012. [Online]. Available: http://jlt.osa.org/abstract.cfm?URI=jlt-30-10-1524

[9] A. Mecozzi and R.-J. Essiambre, "Nonlinear Shannon Limit in Pseudolinear Coherent Systems," *J. Lightwave Technol.*, vol. 30, no. 12, pp. 2011–2024, Jun 2012. [Online]. Available: http://jlt.osa.org/abstract.cfm?URI=jlt-30-12-2011

[10] M. Secondini and E. Forestieri, "Analytical Fiber-Optic Channel Model in the Presence of Cross-Phase Modulation," *IEEE Photonics Technology Letters*, vol. 24, no. 22, pp. 2016–2019, Nov 2012.

[11] P. Johannisson and M. Karlsson, "Perturbation Analysis of Nonlinear Propagation in a Strongly Dispersive Optical Communication System," *J. Lightw. Technol.*, vol. 31, no. 8, pp. 1273–1282, April 2013.

[12] R. Dar *et al.*, "Properties of nonlinear noise in long, dispersion-uncompensated fiber links," *Opt. Express*, vol. 21, no. 22, pp. 25 685–25 699, Nov 2013. [Online]. Available: http://www.opticsexpress.org/abstract.cfm?URI=oe-21-22-25685

[13] P. Serena and A. Bononi, "An Alternative Approach to the Gaussian Noise Model and its System Implications," *J. Lightwave Technol.*, vol. 31, no. 22, pp. 3489–3499, Nov 2013. [Online]. Available: http://jlt.osa.org/abstract.cfm?URI=jlt-31-22-3489

[14] M. Secondini, E. Forestieri, and G. Prati, "Achievable Information Rate in Nonlinear WDM Fiber-Optic Systems With Arbitrary Modulation Formats and Dispersion Maps," *J. Lightwave Technol.*, vol. 31, no. 23, pp. 3839–3852, Dec 2013. [Online]. Available: http://jlt.osa.org/abstract.cfm?URI=jlt-31-23-3839

[15] P. Poggiolini *et al.*, "The GN-Model of Fiber Non-Linear Propagation and its Applications," *J. Lightwave Technol.*, vol. 32, no. 4, pp. 694–721, Feb 2014. [Online]. Available: http://jlt.osa.org/abstract.cfm?URI=jlt-32-4-694

[16] R. Dar *et al.*, "Accumulation of nonlinear interference noise in fiber-optic systems," *Opt. Express*, vol. 22, no. 12, pp. 14 199–14 211, Jun 2014. [Online]. Available: http://www.opticsexpress.org/abstract.cfm?URI=oe-22-12-14199

[17] V. Curri *et al.*, "Extension and validation of the GN model for non-linear interference to uncompensated links using Raman amplification," *Opt. Express*, vol. 21, no. 3, pp. 3308–3317, Feb 2013. [Online]. Available: http://www.opticsexpress.org/abstract.cfm?URI=oe-21-3-3308

[18] ——, "Design Strategies and Merit of System Parameters for Uniform Uncompensated Links Supporting Nyquist-WDM Transmission," *J. Lightwave Technol.*, vol. 33, no. 18, pp. 3921–3932, Sep 2015. [Online]. Available: http://jlt.osa.org/abstract.cfm?URI=jlt-33-18-3921

[19] P. Poggiolini *et al.*, "The LOGON Strategy for Low-Complexity Control Plane Implementation in New-Generation Flexible Networks," in *Optical Fiber Communication Conference/National Fiber Optic Engineers Conference 2013*. Optical Society of America, 2013, p. OW1H.3. [Online]. Available: http://www.osapublishing.org/abstract.cfm?URI=OFC-2013-OW1H.3

[20] R. Pastorelli *et al.*, "Network Planning Strategies for Next-Generation Flexible Optical Networks," *J. Opt. Commun. Netw.*, vol. 7, no. 3, pp. A511–A525, Mar 2015. [Online]. Available: http://jocn.osa.org/abstract.cfm?URI=jocn-7-3-A511

[21] Cisco, "Cisco Visual Networking Index: Forecast and Methodology, 2015-2020," Tech. Rep., 2016.

[22] G. Wellbrock and T. Xia, "How will optical transport deal with future network traffic growth?" in *Optical Communication (ECOC), 2014 European Conference on*, Sept 2014, pp. 1–3.

[23] R.-J. Essiambre *et al.*, "Capacity Limits of Optical Fiber Networks," *J. Lightwave Technol.*, vol. 28, no. 4, pp. 662–701, Feb 2010. [Online]. Available: http://jlt.osa.org/abstract.cfm?URI=jlt-28-4-662

[24] M. Cantono, R. Gaudino, and V. Curri, "Data-rate figure of merit for physical layer in fixed-grid reconfigurable optical networks," in *Optical Fiber Communication Conference*. Optical Society of America, 2016, p. Tu3F.3.

[25] ——, "Potentialities and Criticalities of Flexible-Rate Transponders in DWDM Networks: A Statistical Approach," *J. Opt. Commun. Netw.*, vol. 8, no. 7, pp. A76–A85, Jul 2016. [Online]. Available: http://jocn.osa.org/abstract.cfm?URI=jocn-8-7-A76

[26] ——, "A statistical analysis of transparent optical networks comparing merit of fiber types and elastic transceivers," in *2016 18th International Conference on Transparent Optical Networks (ICTON)*, July 2016, pp. 1–4.

[27] V. Curri, M. Cantono, and R. Gaudino, "Elastic all-optical networks: a new paradigm enabled by the physical layer. How to optimize network performances?" in *Optical Communication (ECOC), 2016 European Conference on*, Sept 2016, pp. 1–3.

[28] F. P. Guiomar *et al.*, "Hybrid Modulation Formats Enabling Elastic Fixed-Grid Optical Networks," *J. Opt. Commun. Netw.*, vol. 8, no. 7, pp. A92–A100, Jul 2016. [Online]. Available: http://jocn.osa.org/abstract.cfm?URI=jocn-8-7-A92

[29] V. Curri and A. Carena, "Merit of Raman Pumping in Uniform and Uncompensated Links Supporting NyWDM Transmission," *J. Lightw. Technol.*, vol. 34, no. 2, pp. 554–565, Jan 2016.

[30] L. Zhang *et al.*, "Dynamic RMSA in spectrum-sliced elastic optical networks for high-throughput service provisioning," in *Computing, Networking and Communications (ICNC), 2013 International Conference on*, Jan 2013, pp. 380–384.

[31] P. Wright, A. Lord, and S. Nicholas, "Comparison of optical spectrum utilization between flexgrid and fixed grid on a real network topology," in *Optical Fiber Communication Conference and Exposition (OFC/NFOEC), 2012 and the National Fiber Optic Engineers Conference*, March 2012, pp. 1–3.

[32] H. Dai, Y. Li, and G. Shen, "Explore Maximal Potential Capacity of WDM Optical Networks Using Time Domain Hybrid Modulation Technique," *J. Lightw. Technol.*, vol. 33, no. 18, pp. 3815–3826, Sept 2015.